RSC Advances

PAPER



Cite this: *RSC Adv.*, 2018, **8**, 40962

# Tungstic acid-functionalized $Fe_3O_4$@$TiO_2$: preparation, characterization and its application for the synthesis of pyrano[2,3-*c*]pyrazole derivatives as a reusable magnetic nanocatalyst†

Jamileh Etemad Gholtash and Mahnaz Farahi *

Received 17th August 2018
Accepted 5th November 2018

DOI: 10.1039/c8ra06886k

rsc.li/rsc-advances

A new magnetic nanocatalyst based on the immobilization of tungstic acid onto 3-chloropropyl-grafted $TiO_2$-coated $Fe_3O_4$ nanoparticles ($Fe_3O_4$@$TiO_2$@$(CH_2)_3OWO_3H$) was prepared, characterized, and applied for the synthesis of pyrano[2,3-*c*]pyrazole derivatives. The characterization was performed using FT-IR spectroscopy, X-ray diffraction (XRD), scanning electron microscopy (SEM), energy-dispersive X-ray spectroscopy (EDS), and vibrating sample magnetometry (VSM) analysis. Pyranopyrazoles were synthesized in the presence of this novel catalyst *via* a three-component reaction of 3-methyl-1-phenyl-2-pyrazolin-5-one, malononitrile, and aromatic aldehydes with high yields. It is a low cost, nontoxic and thermally stable catalyst, which shows a long life and can be reused for several catalytic cycles without deactivation or selectivity loss.

## Introduction

Despite the many benefits of homogeneous catalysts such as high activity and selectivity, heterogeneous catalytic systems have surpassed them due to the high capability for recycling and reutilization.[1] Over the past century, nanocatalysts as a bridge between heterogeneous and homogeneous catalysis have drawn great attention for application in different fields. The significant advantage of nanoparticles is their high specific surface area to volume ratio leading to increase in the contact with the reactants.[2–4] They also have many other advantages such as presence of various surface reactive sites, high activity, selectivity, and desired resilience, which make them recognized as a pioneering technology in green chemistry.[5] Despite the several mentioned benefits of nanomaterials, they are difficult to separate. Therefore, it is important to design recoverable and well-dispersed nanocatalysts.

Recently, $Fe_3O_4$ magnetite nanoparticles (MNPs) have been intensively used as catalytic supports owing to the facility of isolation from the reaction mixture using an external magnet. Furthermore, these systems possess highly potential active sites for loading of other functional groups to prepare novel heterogeneous catalysts.[6–11] To prevent $Fe_3O_4$ nanoparticles from oxidation in an air atmosphere and in order to increase the surface area and simplify the surface functionalization, a protective shell can be formed on their surface.[12]

$TiO_2$ have been successfully applied as a nontoxic, low cost and highly effective catalyst that has good mechanical resistance and stability in acidic and oxidative environments. $TiO_2$ was also found to be a good support material for heterogeneous catalysis due to the strong metal support interaction, chemical stability, and acid–base property.[13–15] Because of the small size of $TiO_2$ particles and difficulties in the separation of catalyst from the reaction media, there are some significant drawbacks in using $TiO_2$ as a heterogeneous catalyst. Immobilization of $TiO_2$ on magnetic nanoparticles as suitable alternative supports to produce magnetically recoverable heterogeneous catalysts allows a convenient recovery of magnetic catalyst under an external magnetic field.[16,17]

In recent years, there has been increasing attention in the synthesis of pyrano[2,3-*c*]pyrazoles as an important class of heterocyclic compounds.[18–21] This interest has resulted from their vital biological activities such as analgesic, antitumor, anticancer, and anti-inflammatory as well as their potential as inhibitors of human Chk1 kinase.[22,23] The pyrano[2,3-*c*]pyrazoles subunit is present in various pharmaceutical and medicinally useful molecules.[24] They are also the main building blocks in the synthesis of natural products as well as in heterocyclic compounds.[25]

Taking the above facts into consideration and in continuation of our research on the synthesis of heterogeneous catalysts,[26–31] in this study, we have immobilized tungstic acid on $TiO_2$-coated $Fe_3O_4$ magnetic nanoparticles ($Fe_3O_4$@$TiO_2$@$(CH_2)_3OWO_3H$) and then investigated its performance as a novel strong, recoverable, and stable acid nanocatalyst for synthesis of pyrano[2,3-*c*]pyrazole derivatives.

*Department of Chemistry, Yasouj University, Yasouj, Iran, 75918-74831. E-mail: farahimb@yu.ac.ir; Fax: (+98) 7412242167*

† Electronic supplementary information (ESI) available. See DOI: 10.1039/c8ra06886k

## Experimental

Chemicals were purchased from Fluka, Merck and Aldrich chemical companies. Known products were identified *via* comparison of their structural data and physical properties with their reported data in the literature. Melting points were determined by an electrothermal kSB1N apparatus. Fourier transform infrared (FT-IR) spectra were recorded on a Shimadzu-470 spectrometer using KBr pellets. The morphology of the particles was observed by scanning electron microscopy (SEM) under acceleration voltage of 26 kV. X-ray powder diffraction (XRD) patterns were recorded using a Bruker AXS (D8 Advance) X-ray diffractometer with Cu Kα radiation ($\lambda = 0.15418$ nm). Energy dispersive spectroscopy (EDS) was obtained using TESCAN Vega model instrument. The magnetic measurement was carried out in a vibrating sample magnetometer (VSM; Kashan university, Kashan, Iran) at room-temperature.

### Preparation of $Fe_3O_4$ MNPs

A solution of $FeCl_2 \cdot 4H_2O$ (1 g, 5 mmol) and $FeCl_3 \cdot 6H_2O$ (2.7 g, 10 mmol) (dissolved in 45 mL double distilled water) was degassed with an argon gas, heated to 80 °C and stirred for 30 minutes. Then, sodium hydroxide solution (5 mL, 10 M) was slowly added dropwise. After stirring at 80 °C for 1 h under argon atmosphere, $Fe_3O_4$ MNPs was separated by an external magnet and washed with double distilled water until pH 9 and then dried at 60 °C.[32]

### Synthesis of nano-$Fe_3O_4$@$TiO_2$

The prepared $Fe_3O_4$ MNPs were dispersed in a mixture of absolute ethanol and acetonitrile (125 : 45 mL) by sonication for 20 min. Then, ammonia aqueous solution (0.75 mL, 25%) was added under vigorous stirring for 30 minutes. After that, tetraethyl orthotitanate (TEOT) (1.5 mL) dissolved in absolute ethanol (20 mL) was slowly added to the above suspension, under continuous mechanical stirring at 30 °C. This mixture was stirred for 1.5 h to obtain nano-$Fe_3O_4$@$TiO_2$. The resulting precipitate was collected by an external magnet and washed with absolute ethanol and dried at room-temperature.[33]

### Preparation of $Fe_3O_4$@$TiO_2$@$(CH_2)_3Cl$

A mixture of $Fe_3O_4$@$TiO_2$ (0.2 g) and 3-chloropropyltrimethoxysilane (2 mL) was stirred with an argon gas under reflux conditions for 12 h. Next, the obtained product was separated by a normal magnet and washed using toluene, ethanol–water mixture, and distilled water. Finally, obtained $Fe_3O_4$@$TiO_2$@$(CH_2)_3Cl$ was dried in an oven at 60 °C.

### Preparation of $Fe_3O_4$@$TiO_2$@$(CH_2)_3OWO_3H$ (1)

In the final stage, a mixture of $Fe_3O_4$@$TiO_2$@$(CH_2)_3Cl$ (0.5 g) and $Na_2WO_4 \cdot 2H_2O$ (0.25 g) in DMSO (5 mL) was stirred at reflux under argon atmosphere for 12 h. After cooling, the obtained catalyst was decanted and washed twice with DMSO, once with distilled water, and dried at 60 °C for 6 h. Then, the functionalized magnetic nanoparticles were added to the flask containing HCl (30 mL, 0.1 N) and stirred for 1 h at room-temperature. The resulting catalyst was decanted, washed with DMSO and water, and finally dried in oven at 60 °C for 12 h.

### General procedure for the synthesis of pyranopyrazole derivatives 5

$Fe_3O_4$@$TiO_2$@$(CH_2)_3OWO_3H$ (0.003 g) was added to a mixture of aldehydes (1 mmol), 3-methyl-1-phenyl-2-pyrazolin-5-one (1 mmol), and malononitrile (1 mmol). The mixture was stirred under solvent-free conditions at 80 °C for the requisite time. The reaction progress was screened using TLC. After completion of the reaction, ethanol (5 mL) was added to the reaction mass and the catalyst was collected with an external magnet. Additional purification was achieved by recrystallization from hot ethanol.

**6-Amino-4-(2,4-dihydroxyphenyl)-3-methyl-1-phenyl-1,4-dihydropyrano[2,3-*c*]pyrazole-5-carbonitrile (5q).** White crystals, IR (KBr): $\nu_{max} = 3424, 3309, 3183, 2923, 2854, 2211, 1590, 1511, 1400, 1351, 1255, 1189, 1045, 842, 800$ cm$^{-1}$. $^1$H NMR (400 MHz, DMSO-$d_6$): $\delta = 9.68$ (s, 1H), 7.92 (s, 1H), 7.76 (s, 2H), 7.52–7.75 (m, 2H), 7.25–7.27 (m, 2H), 6.89 (s, 2H), 6.45 (d, 2H, $J = 4$ Hz), 6.32 (s, 1H), 5.53 (s, 1H), 1.82 (s, 3H). $^{13}$C NMR (100 MHz, DMSO-$d_6$): $\delta = 166.61, 162.25, 161.98, 159.71, 155.85, 153.63, 138.27, 126.38, 123.14, 117.11, 114.33, 108.82, 107.09, 103.83, 101.35, 75.76, 42.11, 26.12$. Anal. calcd for $C_{20}H_{16}N_4O_3$: C, 66.66; H, 4.48; N, 15.55. Found: C, 66.58; H, 4.53; N, 15.60.

**6-Amino-4-(5-bromo-2-hydroxyphenyl)-3-methyl-1-phenyl-1,4-dihydropyrano[2,3-*c*]pyrazole-5-carbonitrile (5r).** Yellow crystals, IR (KBr): $\nu_{max} = 3455, 3347, 3212, 2935, 2210, 1646, 1608, 1554, 1477, 1388, 1280, 1222, 1087, 802, 470$ cm$^{-1}$. $^1$H NMR (400 MHz, DMSO-$d_6$): $\delta = 8.71$ (s, 1H), 7.71 (d, 2H, $J = 4$ Hz), 7.52 (t, 2H, $J = 4$ Hz), 7.36 (s, 1H), 7.27–7.30 (m, 2H), 6.83–6.93 (m, 2H), 6.61 (d, 1H, $J = 4$ Hz), 5.46 (s, 1H), 2.04 (s, 3H). $^{13}$C NMR (100 MHz, DMSO-$d_6$): $\delta = 162.97, 162.31, 158.22, 158.17, 151.67, 140.98, 137.22, 127.62, 121.35, 118.38, 118.06, 118.03, 117.24, 116.73, 97.66, 75.22, 47.56, 23.87$. Anal. calcd for $C_{20}H_{15}BrN_4O_2$: C, 56.75; H, 3.57; N, 13.24. Found: C, 56.70; H, 3.51; N, 13.29.

## Results and discussion

$Fe_3O_4$@$TiO_2$@$(CH_2)_3OWO_3H$ (**1**) was prepared following the protocol shown in Scheme 1. Firstly, $Fe_3O_4$ nanoparticles were synthesized *via* coprecipitation method.[32] Subsequently, tetraethyl orthotitanate (TEOT), as a coating agent, reacts with $Fe_3O_4$ to develop $TiO_2$ layer on the $Fe_3O_4$ backbone.[33] The OH groups on the titanium coating magnetic nanoparticles ($Fe_3O_4$@$TiO_2$) can be functionalized with 3-chloropropyltriethoxysilan molecule. Finally, the chloride group was replaced by tungstic acid to prepare $Fe_3O_4$@$TiO_2$@$(CH_2)_3OWO_3H$ (**1**) as a magnetic nanocatalyst. The obtained catalyst was characterized *via* FT-IR, X-ray diffraction patterns (XRD), scanning electron microscopy (SEM), energy-dispersive X-ray spectroscopy (EDS), and vibrating sample magnetometer (VSM) analysis.

Fig. 1 shows the X-ray diffraction (XRD) patterns of the synthesized nano-$Fe_3O_4$@$TiO_2$ and $Fe_3O_4$@$TiO_2$@$(CH_2)_3OWO_3H$

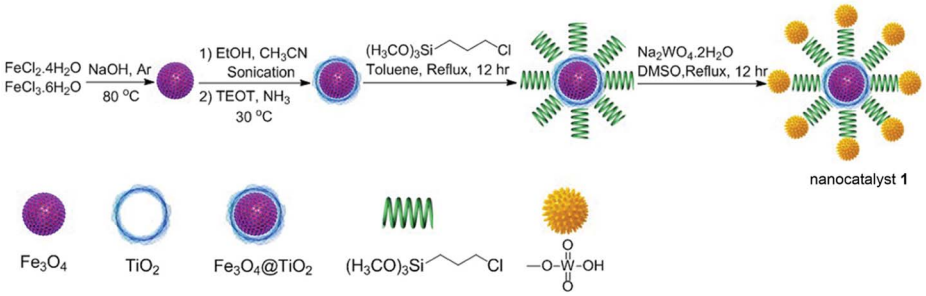


Scheme 1 Preparation of $Fe_3O_4$@$TiO_2$@$(CH_2)_3OWO_3H$ (**1**).

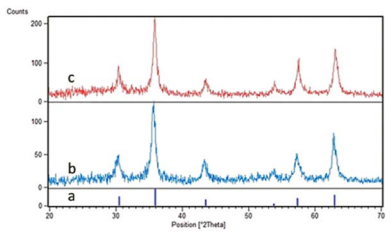


Fig. 1 The XRD patterns of (a) $Fe_3O_4$, (b) $Fe_3O_4$@$TiO_2$, and (c) $Fe_3O_4$@$TiO_2$@$(CH_2)_3OWO_3H$.

in the range 20–70°. In Fig. 1c, the following signals at (220), (210), (400), (511), and (440) and $2\theta = 30.10°$, 35.60°, 43.40°, 53.50°, 57.20°, and 62.80 planes confirm that the main formed phase was a cubic $Fe_3O_4$, which is in agreement with the JCPD 79-0417 standard.[34] Also, the mentioned indexes revealed that the new catalyst in Fig. 1c has the similar structure to $Fe_3O_4$ nanoparticles in Fig. 1a, and this shows that no phase change was observed after surface modification of the magnetite nanoparticles. The peak that confirmed the presence of tungstate group appeared in the range of $2\theta = 22°$.[35] The particle size of the prepared catalyst could be approximated using the Debye–Scherrer equation, $D = k\lambda/\beta \cos\theta$, where $D$ is the average crystalline size, $\lambda$ is the X-ray wavelength, $k$ is the Scherrer constant, $\beta$ is the half width of XRD diffraction lines, and $\theta$ is the Bragg diffraction angle. The particle size relevant to the Debye–Scherrer equation was calculated to be 23 nm.

The FT-IR spectra of the $Fe_3O_4$, $Fe_3O_4$@$TiO_2$, $Fe_3O_4$@$TiO_2$@$(CH_2)_3Cl$, and $Fe_3O_4$@$TiO_2$@$(CH_2)_3OWO_3H$ are shown in Fig. 2. The broad peak at about 2600–3700 $cm^{-1}$ could be attributed to the overlapping of OH stretching bands (corresponding to uncoated OH and acidic OH). The presence of characteristic peaks corresponding to Fe–O stretching vibration near 584 $cm^{-1}$ in all compared spectra was a confirmation of how nanostructure of $Fe_3O_4$ was preserved throughout the process. In Fig. 2b, the peaks discerned at 1118 $cm^{-1}$ and 1400 $cm^{-1}$ can be ascribed to the stretching vibration modes of Ti–O and Fe–O–Ti bonds, respectively. In Fig. 2c, $CH_2$ bending, as a broad band and symmetric $CH_2$ and asymmetric $CH_2$ of the alkyl chains appeared at 1480 $cm^{-1}$ and 2860–2923 $cm^{-1}$, respectively. In Fig. 2d, after modification of $Fe_3O_4$@$TiO_2$@$(-CH_2)_3Cl$ with tungstic acid, new bonds appeared at 887 $cm^{-1}$, which corresponded to W=O vibrations (Fig. 3).

Surface morphology of $Fe_3O_4$@$TiO_2$@$(CH_2)_3OWO_3H$ was observed *via* scanning electron microscopy (SEM). The result demonstrates that the sample consists of homogeneous spherical nanoparticles with diameters in the range of 33.79–90.72 nm (Fig. 4).

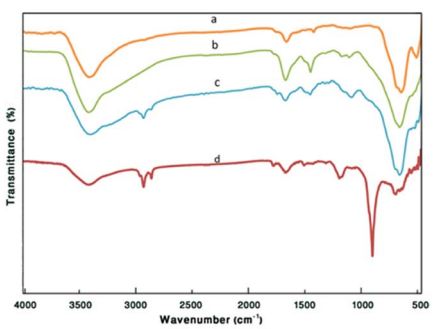


Fig. 2 The FT-IR spectra of (a) $Fe_3O_4$ MNPs, (b) $Fe_3O_4$@$TiO_2$, (c) $Fe_3O_4$@$TiO_2$@$(CH_2)_3Cl$, and (d) $Fe_3O_4$@$TiO_2$@$(CH_2)_3OWO_3H$.

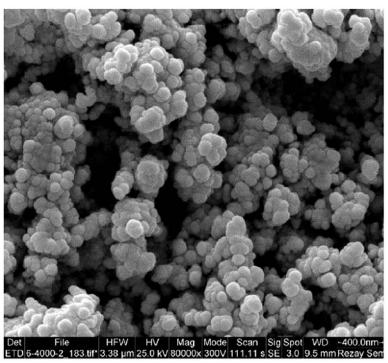


Fig. 3 The SEM image of catalyst **1**.

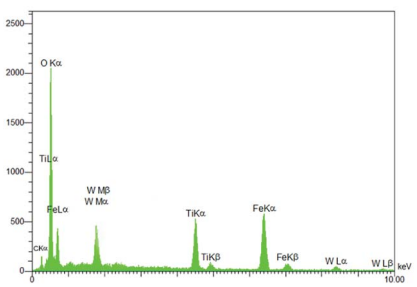


Fig. 4 EDS analysis of $Fe_3O_4$@$TiO_2$@$(CH_2)_3OWO_3H$.

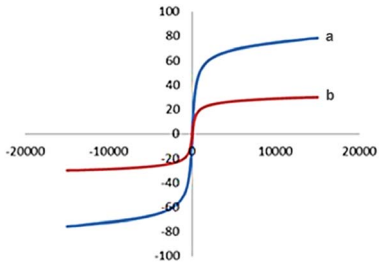


Fig. 5 Room-temperature magnetization curves of (a) $Fe_3O_4$@$TiO_2$ and (b) $Fe_3O_4$@$TiO_2$@$(CH_2)_3OWO_3H$.

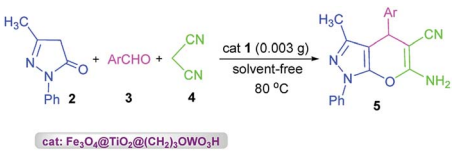


Scheme 2 Synthesis of pyranopyrazoles **5** in the presence of nano-catalyst **1**.

Energy-dispersive X-ray spectroscopy (EDS) was used for the structural characterization of $Fe_3O_4$@$TiO_2$@$(CH_2)_3OWO_3H$. As can be seen in Fig. 4, the components of this catalyst included Fe, Ti, O, C and W, which indicate the acceptable concordance with the expectations and also confirm the successful incorporation of tungstate groups.

The vibrating sample magnetometer (VSM) was applied to evaluate the magnetic measurement of the prepared catalyst (Fig. 5). In the present method, the magnetic behavior of the above catalyst has been calculated by drawing the hysteresis loops at room-temperature. The below magnetization curves shows the saturation magnetization of $Fe_3O_4$@$TiO_2$ nanoparticles and $Fe_3O_4$@$TiO_2$@$(CH_2)_3OWO_3H$, which were diminished to 23.4 emu $g^{-1}$ from 65.8 emu $g^{-1}$ for $Fe_3O_4$@$TiO_2$. As can be seen, the difference of saturation magnetization between $Fe_3O_4$@$TiO_2$ nanoparticles and $Fe_3O_4$@$TiO_2$@$(CH_2)_3OWO_3H$ was small.

Table 1 Optimization of the model reaction

| Entry | Solvent | Catalyst (g) | $T$ (°C) | Time (h) | Yield[a] (%) |
|---|---|---|---|---|---|
| 1 | EtOH | 0.005 | Reflux | 180 | 52 |
| 2 | $CHCl_3$ | 0.005 | Reflux | 180 | 50 |
| 3 | Toluene | 0.005 | Reflux | 180 | 45 |
| 4 | $H_2O$ | 0.005 | Reflux | 180 | 40 |
| 5 | $CH_3CN$ | 0.005 | Reflux | 180 | 40 |
| 6 | MeOH | 0.005 | Reflux | 180 | 50 |
| 7 | — | 0.005 | 60 | 180 | 70 |
| 8 | — | 0.005 | 80 | 120 | 75 |
| 9 | — | 0.005 | 100 | 120 | 75 |
| 10 | — | 0.004 | 80 | 120 | 80 |
| 11 | — | 0.003 | 80 | 75 | 90 |
| 12 | — | 0.003 | 100 | 75 | 85 |
| 13 | — | 0.003 | 110 | 75 | 80 |
| 14 | — | 0.007 | 80 | 75 | 85 |

[a] Isolated yields.

Table 2 $Fe_3O_4$@$TiO_2$@$(CH_2)_3OWO_3H$-catalyzed synthesis of pyrano[2,3-*c*]pyrazoles **5**[a]

| Entry | Ar | Time (min) | Yield[b] (%) | Mp (°C) |
|---|---|---|---|---|
| **5a** | $C_6H_5$ | 75 | 90 | 170–172 (ref. 36) |
| **5b** | 4-$OCH_3C_6H_4$ | 90 | 87 | 174–175 (ref. 36) |
| **5c** | 2,4-$Cl_2C_6H_3$ | 80 | 84 | 185–186 (ref. 36) |
| **5d** | 4-$ClC_6H_4$ | 70 | 90 | 172–174 (ref. 36) |
| **5e** | 2-$BrC_6H_4$ | 82 | 78 | 166–167 (ref. 17) |
| **5f** | 3-$ClC_6H_4$ | 85 | 86 | 157–159 (ref. 17) |
| **5g** | 2-$ClC_6H_4$ | 80 | 89 | 144–146 (ref. 36) |
| **5h** | 4-$NO_2C_6H_4$ | 70 | 79 | 194–196 (ref. 36) |
| **5k** | 4-$C_3H_7C_6H_4$ | 90 | 88 | 169–170 (ref. 36) |
| **5l** | 4-$BrC_6H_4$ | 77 | 78 | 183–184 (ref. 36) |
| **5m** | 4-$OHC_6H_4$ | 95 | 92 | 211–212 (ref. 36) |
| **5n** | 4-($PhCH_2O$) $C_6H_4$ | 100 | 80 | 160–161 (ref. 36) |
| **5p** | 3-$OC_2H_5$ 4-OH $C_6H_3$ | 95 | 83 | 169–171 (ref. 36) |
| **5q** | 2,4-$(OH)_2$ $C_6H_3$ | 110 | 80 | 320–321[c] |
| **5r** | 5-Br 2-OH $C_6H_3$ | 120 | 83 | 314–315[c] |

[a] Reaction conditions: 3-methyl-1-phenyl-2-pyrazolin-5-one (1 mmol), arylaldehyde (1 mmol), malononitrile (1 mmol), and $Fe_3O_4$@$TiO_2$@$(CH_2)_3OWO_3H$ (0.003 g), 80 °C. [b] Isolated yields. [c] Novel product.

After full structural characterization of nano-$Fe_3O_4$@$TiO_2$@$(CH_2)_3OWO_3H$, it has been successfully applied to synthesis of pyrano[2,3-*c*]pyrazole derivatives **5** *via* a three-


Fig. 6 Reusability of catalyst **1** in the reaction between 3-methyl-1-phenyl-2-pyrazolin-5-one, malononitrile, and benzaldehyde.

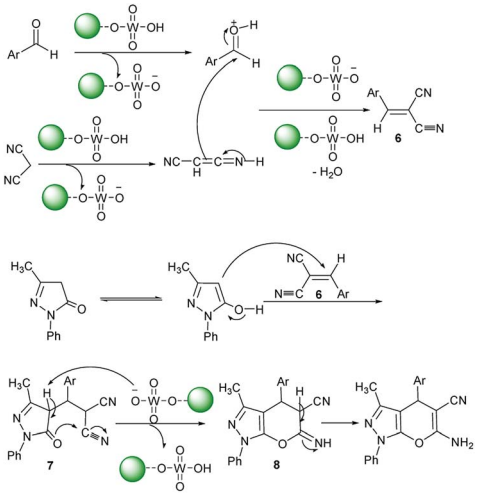


Scheme 3 Proposed mechanism for the synthesis of product **5** catalyzed by catalyst **1**.

Table 3 Comparison of the results for the synthesis of **5a** by other catalysts

| Entry | Catalyst | Catalyst loading | Condition | Time (min)/yield[a] (%) |
|---|---|---|---|---|
| 1 | Piperidine | 0.05 mL | EtOH, MW | 8/61 (ref. 37) |
| 2 | γ-Alumina | 30 mol% | $H_2O$, reflux | 50/80 (ref. 38) |
| 3 | Mg/Al HT | 0.1 g | EtOH, r.t. | 60/87 (ref. 39) |
| 4 | *p*-Toluene sulfonic acid | 0.05 g | $H_2O$, reflux | 55/86 (ref. 40) |
| 5 | Triethylbenzylammonium chloride | 0.15 g | $H_2O$, 90 °C | 360/99 (ref. 41) |
| 6 | Catalyst **1** | 0.003 g | 80 °C, solvent-free | 75/90[b] |

[a] Isolated yields. [b] This study.

component reaction of 3-methyl-1-phenyl-2-pyrazolin-5-one **2**, aromatic aldehydes **3**, malononitrile **4** under solvent-free conditions (Scheme 2).

In order to find the most appropriate reaction conditions, the reaction of 3-methyl-1-phenyl-2-pyrazolin-5-one (1 mmol), benzaldehyde (1 mmol), and malononitrile (1 mmol) was selected as a model reaction. The desired product was not produced in the absence of a catalyst even after a long reaction time. Then, we attempted with different amounts of $Fe_3O_4$@$TiO_2$@$(CH_2)_3OWO_3H$ as catalyst under various conditions. The obtained data for several catalyst loads, temperatures, and solvents are summarized in Table 1. It was seen that the selection of 0.003 g of catalyst **1** at 80 °C under solvent-free conditions would be the best of choice (Table 1, entry 11).

Under these conditions, a range of aryl aldehydes, containing both electron-donating and electron-withdrawing groups were examined and resulted in good to excellent yields of the products in short reaction times (Table 2).

Due to the importance of recoverability and recyclability of the catalyst from both practical and economical viewpoints, we next examined the reusability of $Fe_3O_4$@$TiO_2$@$(CH_2)_3OWO_3H$ in the reaction of 3-methyl-1-phenyl-2-pyrazolin-5-one, benzaldehyde, and malononitrile under optimized reaction conditions. $Fe_3O_4$@$TiO_2$@$(CH_2)_3OWO_3H$ was separated by a permanent magnet from the reaction mixture, washed with methanol, and reused in the next run without further treatment. The results revealed that the catalyst could be reused for five cycles without remarkable loss in catalytic performance. The data are exhibited in Fig. 6.

The proposed formation mechanism of product **5** is given in Scheme 3. Initially, intermediate **6** was formed *via* the condensation of activated aromatic aldehydes and malononitrile in the presence of acid catalyst **1**. It is reasonable to suppose that the intermediate **6** was attached by *c*-4 of 3-methyl-1-phenyl-2-pyrazolin-5-one which rearranged into intermediate **7**. Cyclization of **7** by the nucleophilic attack of C=O group on the cyano moiety gives **8**. Finally, a sequence of tautomerization of **8** generates the related product.

The major advantages of the presented protocol over existing methods can be seen by comparing our results with those of some recently reported procedures, as shown in Table 3.

## Conclusions

In this study, we have introduced for the first time a green and recyclable nanomagnetic solid acid catalyst, namely $Fe_3O_4$@$TiO_2$@$(CH_2)_3OWO_3H$. Structural verification was performed using FT-IR, XRD, SEM, EDS and VSM. This novel $Fe_3O_4$-based heterogeneous nanocatalyst was successfully used for the synthesis of pyrano[2,3-*c*]pyrazoles. Besides recyclability, its advantages like operational simplicity, good chemical yields combined with step- and atom-economic aspects are the main promising points of this study which make this strategy highly attractive.

## Conflicts of interest

There are no conflicts to declare.

## Acknowledgements

The authors gratefully acknowledge partial support of this study by Yasouj University, Iran.

## Notes and references

1 M. A. Zolfigol and M. Yarie, *Appl. Organomet. Chem.*, 2017, **31**, 3598.
2 S. Shylesh, V. Schünemann and W. R. Thiel, *Angew. Chem., Int. Ed.*, 2010, **49**, 3428.
3 B. Karimi, F. Mansouri and H. M. Mirzaei, *ChemCatChem*, 2015, **7**, 1736.
4 B. K. Khosravian and M. Farahi, *New J. Chem.*, 2017, **41**, 11584.
5 R. K. Sharma, S. Sharma, S. Dutta, R. Zboril and M. B. Gawande, *Green Chem.*, 2015, **17**, 3207.
6 H. Woo, K. Lee, S. Park and K. H. Park, *Molecules*, 2014, **19**, 699.
7 R. Hudson, Y. Feng, R. S. Varma and A. Moores, *Green Chem.*, 2014, **16**, 4493.
8 M. B. Gawande, P. S. Branco and R. S. Varma, *Chem. Soc. Rev.*, 2013, **42**, 3371.
9 J. Safari and Z. Zarnegar, *RSC Adv.*, 2015, **5**, 17738.
10 H. Kefayati, M. Golshekan, S. Shariati and M. Bagheri, *Chin. J. Catal.*, 2015, **36**, 572.

 

11 J. S. Yoo, *Catal. Today*, 1998, **44**, 27.
12 L. Tan, X. Zhang, Q. Liu, J. Wang, Y. Sun, X. Jing, J. Liu, D. Songa and L. Liuc, *Dalton Trans.*, 2015, **44**, 6909.
13 Q. J. Xiang, K. L. Lv and J. G. Yu, *Appl. Catal., B*, 2010, **96**, 557.
14 X. Yu, S. Liu and J. Yu, *Appl. Catal., B*, 2011, **104**, 12.
15 M. Abbas, B. P. Raoc, V. Reddy and C. Kim, *Appl. Catal., B*, 2009, **89**, 527.
16 W. P. Kwan and B. M. Voelker, *Environ. Sci. Technol.*, 2003, **37**, 1150.
17 R. Sharifi Aliabadi and N. O. Mahmoodi, *RSC Adv.*, 2016, **6**, 85877.
18 A. R. Moosavi-Zare, M. A. Zolfigol and A. Mousavi-Tashar, *Res. Chem. Intermed.*, 2016, **42**, 7305.
19 R. Sharifi Aliabadi and N. O. Mahmoodi, *RSC Adv.*, 2016, **6**, 85877.
20 G. Vasuki and K. Kumaravel, *Tetrahedron Lett.*, 2008, **49**, 5636.
21 G. M. Reddy and J. R. Garcia, *J. Heterocycl. Chem.*, 2017, **54**, 89.
22 M. N. Nasr and M. M. Gineinah, *Arch. Pharm.*, 2002, **335**, 289.
23 S. A. El-Assiery, G. H. Sayed and A. Fouda, *Acta Pharm.*, 2004, **54**, 143.
24 X. H. Yang, P. H. Zang, Z. M. Wang, F. Jing and Y. H. Zhou, *Ind. Crops Prod.*, 2014, **52**, 413.
25 M. Farahi, M. Davoodi and M. Tahmasebi, *Tetrahedron Lett.*, 2016, **57**, 1582.
26 M. Farahi, F. Tamaddon, B. Karami and S. Pasdar, *Tetrahedron Lett.*, 2015, **56**, 1887.
27 M. Farahi, B. Karami, R. Keshavarz and F. Khosravian, *RSC Adv.*, 2017, **7**, 46644.
28 H. Mohamadi Tanuraghaj and M. Farahi, *RSC Adv.*, 2018, **8**, 27818.
29 M. Farahi, B. Karami, Z. Banaki, F. Rastgoo and K. Eskandari, *Monatsh. Chem.*, 2017, **148**, 1469.
30 S. Akrami, B. Karami and M. Farahi, *RSC Adv.*, 2017, **7**, 34315.
31 M. C. Mascolo, Y. Pei and T. A. Ring, *Materials*, 2013, **6**, 5549.
32 F. Nemati, M. Heravi and A. Elhampour, *RSC Adv.*, 2015, **5**, 45775.
33 A. Amoozadeh, S. Golian and S. Rahimi, *RSC Adv.*, 2015, **5**, 45974.
34 C. Santato, M. Odziemlowski, M. Ulmann and J. Augustynski, *J. Am. Chem. Soc.*, 2001, **123**, 10639.
35 M. Farahi, B. Karami, I. Sedighimehr and H. Mohamadi Tanuraghaj, *Chin. Chem. Lett.*, 2014, **25**, 1580.
36 G. M. Reddy and J. R. Garcia, *J. Heterocycl. Chem.*, 2017, **54**, 89.
37 J. F. Zhou, S. J. Tu, H. Q. Zhu and S. J. Zhi, *Synth. Commun.*, 2002, **32**, 3363.
38 H. Mecadon, M. R. Roham, M. Ranjbangshi and B. Myrbon, *Tetrahedron Lett.*, 2011, **52**, 2523.
39 S. W. Kshirsagar, N. R. Patil and S. D. Samant, *Synth. Commun.*, 2011, **41**, 1320.
40 M. M. Heravi, N. Javanmard, H. A. Oskooi and B. Baghernejad, *Gazi University Journal of Science*, 2011, **24**, 227.
41 M. M. Heravi, A. Ghods, F. Derikvand, K. Bakhtiari and F. F. Bamoharram, *J. Iran. Chem. Soc.*, 2010, **7**, 615.